Article

Numerical Dolly Rollover Evaluation Using a Damping-Harmonic System with a Low Back Booster to Reduce Injuries in a Six-Year-Old Child

Ivan Lenin Cruz-Jaramillo [1], José Luis Torres-Ariza [2], Mario Alberto Grave-Capistrán [2],
Elliot Alonso Alcántara-Arreola [2], Carlos Alberto Espinoza-Garcés [2] and Christopher René Torres-SanMiguel [2,*]

1 Departamento de Investigación y Desarrollo Tecnológico, Tecnológico de Estudios Superiores de Tianguistengo, Km 22. Carretera Tenango-La Marquesa Santiago Tilapa, Santiago Tianguistenco 52650, Mexico
2 Instituto Politécnico Nacional, Escuela Superior de Ingeniería Mecánica y Eléctrica Sección de Estudios de Posgrado e Investigación, Unidad Zacatenco Edificio 5, Ciudad de México 07738, Mexico; cespinozag0700@alumno.ipn.mx (C.A.E.-G.)
* Correspondence: ctorress@ipn.mx; Tel.: +52-55-5729-6000 (ext. 54815)

Abstract: This study examined injuries sustained by a six-year-old child dummy in a numerical dolly rollover crash using a Toyota Yaris 2010. A harmonic dynamic system (HDS) composed of spring, dampers, and masses with a Low Back Booster (LBB) is denominated as HDS-LBB model. The HDS-LBB was designed to allow damping movements along three Cartesian axes (X, Y, Z) to reduce the energy transferred to the child by a motor vehicle accident and avoid a high injury risk. The HDS-LBB incorporates springs into the vertical axis to decrease the vertical movement during the rollover. The numerical analysis was conducted using LS-Dyna® R12.1 version during an interval of 1 s, and the boundary conditions were set by the Federal Motor Vehicle Safety Standard (FMVSS) 213 for child restraint recommendations and the FMVSS 208 for a dolly rollover procedure. Data on head and thorax decelerations, neck flexion-extension, and thoracic deflection were acquired at a rate of 1 ms. The injury values obtained by the HDS-LBB were compared with the injury values by another configuration denominated LBB-ISOFIX to assess the effectiveness of the model proposed. The results show a higher peak injury value in the neck and thorax because of seatbelt displacement across the child's shoulder. Nevertheless, despite this seatbelt behavior, the injuries sustained remained below the Injury Assessment Reference Values (IARVS).

Keywords: passive safety; biomechanics; Injury Assessment Reference Values; Low Back Booster; harmonic system; dolly rollover

1. Introduction

Motor vehicle crashes occur due to different variables, such as poorly designed and maintained roads, human errors, and vehicle breakdowns. In Mexico, 46,921 rollover accidents were recorded from 2018 to 2022, an average of 9385 accidents per year [1]. Rollover crashes are complex interaction scenarios between vehicles, passengers, roads, and environmental factors, according to NHTSA (National Highway Traffic Safety Administration) [2]. A rollover is recognized as a severe and dangerous accident that can cause serious injuries, or it may lead to imminent risk of death. The rollover happens when the vehicle flips onto its roof, and the side part about the longitudinal or lateral axis rotates 90 degrees or more with respect to its direction during the crash [3–5]. The dolly rollover test is performed under some regulations according to the country, and the term dolly refers to the dolly fixture (platform) that moves the test vehicle and generates the necessary test speed to initiate the lateral roll [6]. The most common rollover protocols are the Federal Motor Vehicle Safety Standard (FMVSS) 208, the Canada Motor Vehicle Safety Standard

(CMVSS) 220 for buses, cars, heavy trucks, and light trucks, the Regulation No. 111 of the Economic Commission for Europe of the United Nations (UN/ECE) for categories N and O to evaluate the rollover stability and the UN-ECE regulation 66. A rollover crash transmitted a significant amount of kinetic energy to the occupants and the vehicle. Some safety tips can reduce the probability of injury, such as wearing a seatbelt, not overloading the vehicle, and using the seats in a way that is suitable for the occupants.

The rollover test protocol selected is the FMVSS 208. The protocol considers a mobile platform perpendicular to the vehicle direction with an angle inclination of 23 degrees. At the beginning, a constant speed of 30 mph is applied to move the platform, and a subsequent deceleration to 0 m/s over a distance minor to 3 feet is reached to obtain a pulse deceleration of 20 G approximately in 0.04 s [7]. The principal disadvantage of this protocol, according to studies, is that the occupants in rollovers, including children, demonstrate a high risk of death or serious injuries [8]. In motor vehicle crashes, children are the most exposed to suffering injuries due to several factors such as the body anthropometric, the vehicle type, the impact zone on the vehicle, the seat where the child is seated, and the unsafe practice of being seated without following any safety regulations [9–13]. Children's injuries are mainly located at the neck, thorax, and head [14]. Rollover crash data reported a 28% child passenger fatality in the U.S., and some potential variables are necessary to consider, such as age, gender, seating position, use of any restrain system, vehicle type, and speed [14,15]. For rollover, risk analysis shows that the abdomen, head, thorax, and spine are more common injuries for children. The highest probability of injured body regions is the head [16]. Enhancing children's safety is challenging due to the wide range of children's ages, sizes, and different body properties. A Child Restraint System (CRS) offers a way to increase child safety during other types of crashes. The several CRSs available in the market follow the FMVSS 213 or the European UN/ECE R66 or R129 standard. However, these standards evaluate frontal or lateral protection, and the CRS's performance has not been assessed during the rollover crash, so the manufacturers do not test the effectiveness of CRS during a rollover. Some CRS devices have incorporated improvements such as springs or shock absorber mechanics to dissipate energy through the sliding movement coupling systems, while others include new materials to absorb the impact energy [17–23]. The mechanical coupling with the LBB system is a significant proposal to reduce the number of child injuries or fatalities in a variety of crash scenarios. Currently, the proposal model has been tested under frontal and rollover crash scenarios. The proposal system is designed on the principles of a Harmonic Oscillator and follows the requirements established in ISO 13216 (International Organization Standard). Springs (provide restoring force) and dampers (reduce the system velocity) are used through the X, Y, and Z axes to absorb kinetic energy and protect the child's body during the motor vehicle crash [24]. The use of ISO 13216 provides the dimensions and general requirements for anchoring the CRS. The M-coupling was designed in accordance with the standard and did not have any unsafe areas that could lead to injuries due to possible interactions with the vehicle interior.

Considering that the vehicle collision involves a rebound and energy dissipation, a harmonic oscillator is a good model for dissipating the crash energy and avoiding severe injury to the child. There are two main reasons why mechanical parts were used for damping: the first is to decrease or prevent undesired vibrations due to the interactions between the components, and the second is to absorb the crash energy generated by the high movement.

This study aims to determine and characterize the performance of the Harmonic Device System with LBB (HDS-LBB) in a dolly rollover crash test to decrease the risk of injuries for enhancing child protection. A comparative analysis is proposed between the HDS-LBB and the LBB-ISOFIX configuration that was previously evaluated by Cruz et al. [25]. For both child restraint configurations, the Hybrid III 6-year-old F.E. was used. The structure of the paper is organized as follows: in the section titled Material and Methods, we define the boundary conditions applied in the numerical rollover test, the mesh properties, and the assignment of constitutive materials models for the components.

The section titles Results shows the differences in kinematic behavior and injuries obtained in the neck, head, and thorax between the HDS-LBB and the LBB-ISOFIX. The outcomes show that the HDS mechanism offers a good anchor system, such as the ISOFIX.

2. Materials and Methods

The FMVSS 208 standard [7] is used to establish the conditions under which the rollover test will be performed. In this case, the Toyota Yaris 2010 F.E. model developed by George Washington National Crash Analysis Center (NCAC) was used with the following characteristics: 917 parts, 1,480,422 nodes, and 1,514,068 elements divided into 1,250,424 shells, 258,887 solid and 4738 beams elements [26].

A numerical rollover crash test (Figure 1) is established to obtain the acceleration pulses from the vehicle that are used for the simplified test to perform the HDS-LBB Child Restraint proposal (Figure 2). The catapult is designed with the dimensions specified in the FMVSS 208. The tetrahedral mesh applied consists of 10,650 nodes, 6750 elements, and a mesh size of 8 mm. Table 1 shows the parameters for the numerical rollover developed.
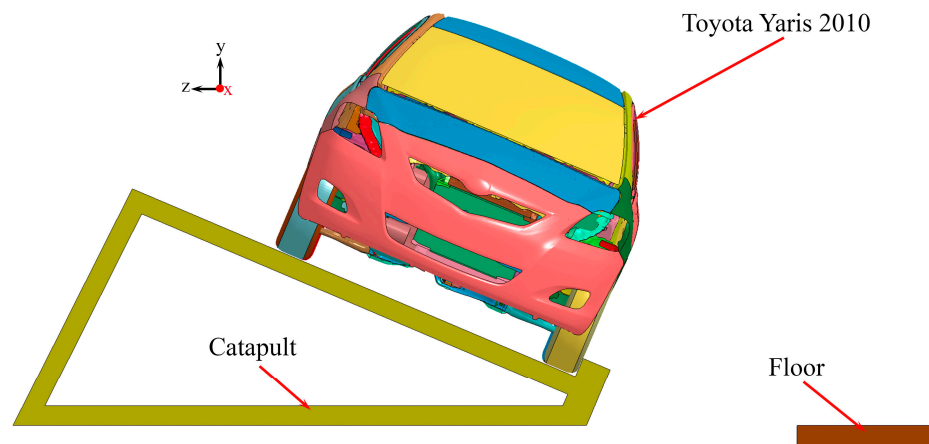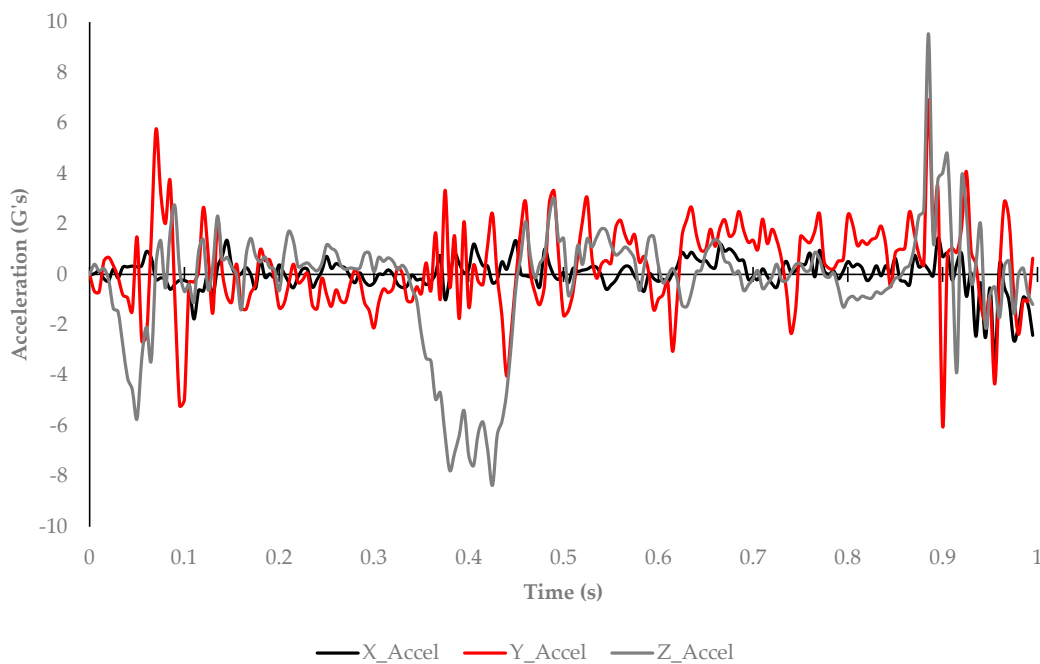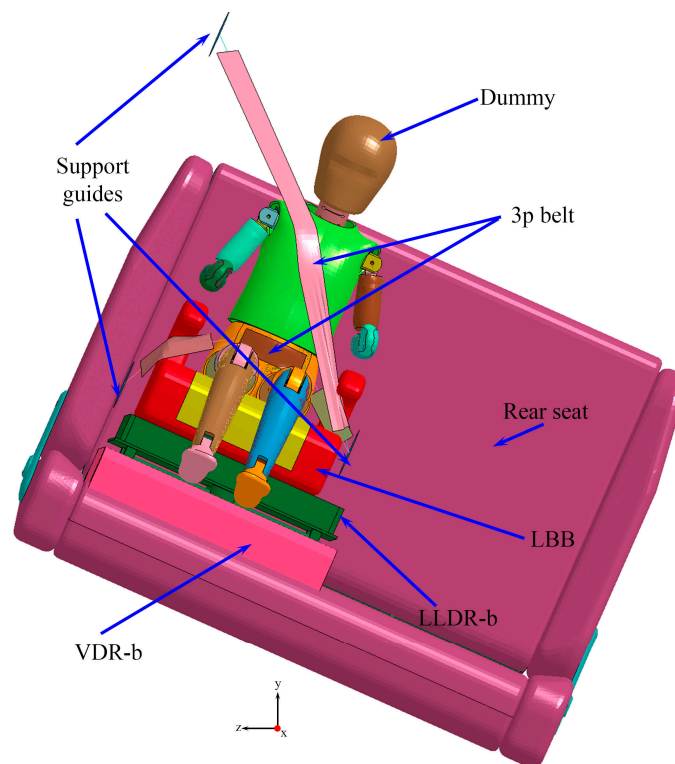

Figure 1. Dolly rollover test.

Figure 2. Acceleration pulses from the numerical rollover test.

Table 1. Numerical rollover test conditions.

Test Speed	13.34 m/s
Time interval	1–1000 ms
Car	Toyota Yaris 2010
Car weight	1100 kg
Roll direction	Right passenger side

The simplified case for the HDS-LBB performance in a rollover test is composed of the vehicle's back seat, a 3-point seatbelt, a LBB, the child model Hybrid III 6yo FE provided under license (Annual license) from LS DYNA® version LSTC_H3_6YO.150202_V0.104.BETA (Figure 3), and the acceleration pulses to represent the vehicle crash behavior during the rollover. The mesh specifications of the model components are summarized in Table 2. From LS-DYNA®, the LS-Prepost version 4.8 was used with the solver version 12.1.

Figure 3. Dolly rollover assembly test setup.

The vehicle's back seat was designed with the accurate dimensions of the Toyota Yaris 2010®. The rear seat consists of 3 parts: steel support, the padding, and the polypropylene connector between the seat back and the seat cushion. All the parts were meshed with a tetrahedral formulation for the seat backrest consisting of 30,852 nodes, 92,118 elements and 183,855 nodes, 827,071 elements for a seat cushion.

The 3-point seatbelt is designed using the Ls-Prepost 4.8 version, which applies unidimensional and bidimensional elements. The seat belt dimensions are 47 mm in width by 1 mm in thickness. For unidimensional (1D) elements, the LS DYNA default configuration for the safety belt was assigned with a mass pull of 5.97×10^{-4} kg/mm [27]. For bidimensional elements, a triangle mesh size is 8 mm, with 667 nodes and 1168 elements. A shell section with a Belytschko–Tsay element formulation with a thickness of 1 mm was selected. Nylon was set with a density of 1×10^{-6} kg/mm^3, a Young's modulus of 5.333 GPa with a yield strength of 0.08 GPa, and 0.3 for Poisson's ratio. Loading and unloading curves to

represent the axial force as a function of the seat belt were implemented [28]. No retractor and pretensioner were applied for the case study.

Table 2. Mesh components properties.

Component	Subcomponent	Mesh Formulation	Type Elements	Element Formulation	Nodes	Elements
LBB	Support material	Tetrahedral	Solid	Constant stress solid element	21,156	92,028
	LBB cushioning	Tetrahedral	Solid	Constant stress solid element	3510	10,028
Seatbelt	Lap belt and shoulder belt	Linear Triangle	Shell (Bidimensional)	Belytschko–Tsay	667	1168
Seat	Steel support	Tetrahedral	Solid	Constant stress solid element	30,852	92,118
	Seat cushioning	Tetrahedral	Solid	Constant stress solid element	183,855	827,071
Harmonic Device System (HDS)	Longitudinal–lateral displacement reduction box (LLDR-b)	Hexahedral	Solid	Constant stress solid element	106,147	69,199
	Vertical displacement reduction box (VDR-b)	Hexahedral	Solid	Constant stress solid element	240,294	208,335

The LBB model is based on the Evenflo® model for groups 2 to 3 (adjustable 3–11 years or 18–49.8 kg). It consists of a support material, in this case, polypropylene, and LBB cushioning with foam DAX 55. The LBB model and the proposal Harmonic Device System components were modeled in SolidWorks® 2021 version and meshed with the LS-Prepost 4.8 version, and the mesh parameters are shown in Table 2.

The child model Hybrid III 6yo FE was proposed to measure child injuries because there is no anthropometric test device (ATD) that has been developed to measure child injuries during a dolly rollover test. The Hybrid III 6yo was seated at the rear right seat for the test setup (Figure 2). The six-year-old child ATD statistics for the current model finite element are 199,102 nodes, 172,328 elements divided into 45,032 shells, 127,154 solid, and 142 beams elements, and the model is released under the units form of mm, ms, kg, and kN.

2.1. Harmonic Dynamic System Setup

The Harmonic Dynamic System (HDS) objective is to decrease the energy transferred from the crash to the child through the harmonic mechanisms proposed. The HDS was designed to reduce the energy not only during a rollover but also to decrease the transferred energy by crash scenarios such as frontal, rear, and lateral. The mechanism was designed with a set of springs and shock absorbers, which allow displacements in the 3 cartesian axes (X, Y, Z). The HDS was designed according to the FMVSS 213 standard and UN/ECE R129 [29], allowing it to adjust adequately to the seat car and the CRS available in the market [29,30]. The proposal is made up of two parts: The longitudinal–lateral displacement reduction box (LLDR-b) and the vertical displacement reduction box (VDR-b). The HDS was previously performed in a frontal crash test by Cruz et al. [18].

The LLDR-b is composed of eight springs for the *x*-axis and four for the *z*-axis, four dampers divided into pairs of two for the X and Z axes, and two mass concentrators. Springs and dampers are proposed to allow CRS displacements in a controlled and damped way. The mass concentrator is implemented to help reduce oscillations that the child and CRS would suffer during the crash. A riel (T) is proposed to allow the displacement for the mass concentrators (M1 and M2) and attach into the *x*-axis a bearing on which the CRS (C) is mounted. The riel is fixed to the bearings (J1 and J2) to allow displacement along the *z*-axis (Figure 4).

The VDR-b consists of two shock absorbers (diagonally arranged and connected to the housing) locked with the LLDR-b through the latch. Additionally, two springs collocated parallel to the *y*-axis are assembled with the LLDR-b. The VDR-b incorporates an adaptative orientation anchor system to make the anchored process more accessible according to the vehicle seat and allow the adaption of the CRS assembly according to the child's age. An arrangement of rods and latches achieves this adaptive anchored process with three L-shaped rods, two placed in the same direction and one opposite to both. The latches are designed in a way that the rod presses the latch with the shorter part, while the longer

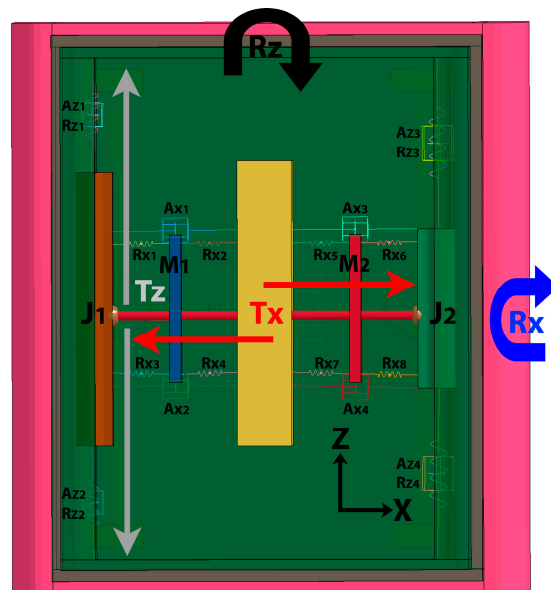part goes through the VDR-b. This interchangeability allows the ISOFIX orientation to be changed (Figure 5).

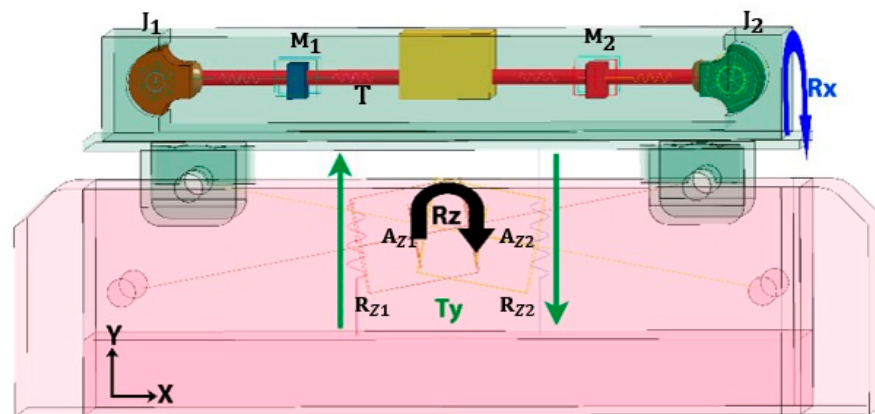**Figure 4.** The longitudinal–lateral displacement reduction box (LLDR-b).

Figure 5. The vertical displacement reduction box (VDR-b).

2.2. Boundary Conditions

The numerical dolly rollover crash test analysis was performed using LS-Dyna®. The mechanical properties and the constitutive model used in LS-Dyna® are shown in Table 3 according to the component and subsystem from the HDS-LBB. The rear seat support, the L-shaped rods, the support guide, and the catapult are assigned with steel. Polypropylene was used for the LBB structure and the connector. Foam DAX 55 was selected for seat and LBB cushioning. The foam material was chosen to avoid an indirect effect (structural materials are more stiffness) during the interaction child-seat.

J1, J2, C, and T parts from the LLDR-b and VDR-b use the mechanical properties of aluminum 1100-H14. M1 and M2 parts implemented structural ASTM A36 steel. Table 4 shows the spring and damper characteristics based on commercial catalogs. Concrete was considered a rigid body, and a rigid constitutive material was modeled since only the vehicle's structure was of interest, and the concrete generation or propagation of microcracks was not significant for the rollover test.

Table 3. Material properties.

Material	Constitutive Model Selected in LS-DYNA	Density (kg/mm^3)	Young's Modulus (GPa)	Yield Strength (GPa)	Poisson's Ratio
Steel	RIGID (020)	7.8×10^{-6}	210	0.6	0.3
Polypropylene [31]	ELASTIC (001)	9×10^{-7}	1.35	0.036	0.312
Foam DAX 55 [32]	LOW_DENSITY_FOAM (057)	3.5×10^{-8}	5×10^{-5}	---	0.31
Aluminum 1100-H14 [33]	ELASTIC (001)	2.71×10^{-6}	70	0.095	0.33
ASTM A36 steel [34–36]	PLASTIC_KINEMATIC (003)	7.85×10^{-6}	200	0.25	0.32
Concrete [34]	RIGID (020)	2.38×10^{-6}	29	---	0.15

Table 4. Constants and dimensions for springs and dampers belonging to the mechanical coupling [37,38].

Device	ID	Value	Length (mm)
Dampers $\frac{kNms}{mm}$	$A_{X1}, A_{X2}, A_{X3}, A_{X4}$	0.015	150
	A_{Y1}, A_{Y2}	0.015	100
	A_{Y3}, A_{Y4}	0.015	150
	A_{Z1}, A_{Z2}	0.04	250
Springs $\frac{kN}{mm}$	$R_{X1}, R_{X2}, R_{X3}, R_{X4}$ $R_{X5}, R_{X6}, R_{X7}, R_{X8}$	1×10^{-5}	50
	R_{Y1}, R_{Y2}	1.5×10^{-5}	100
	R_{Y3}, R_{Y4}	1.5×10^{-5}	150
	R_{Z1}, R_{Z2}	8×10^{-5}	275

The initial velocity is 13.34 m/s along the *Z*-axis. Subsequently, the catapult is decelerated with the curve established in the FMVSS 208 regulation until it reaches the static and the vehicle rollover. The "Y" direction corresponds to the vehicle's vertical direction, and the force applied corresponds to gravity with a constant value of 0.00981 mm/ms². A rigid type of material and a solid section are implemented for the catapult and the ground; since it allows the transmission of energy due to the material properties described, deformations are not considered, focusing the analysis on the structure damages in the vehicle and energy transmission to the vehicle's interior during the rollover. Constraints are set on the nodal elements for the rear seat and the LBB to behave as a single body. The contacts established are shown in Table 5. The CONTACT_AUTOMATIC_SURFACE_TO_SURFACE card was selected to eliminate possible penetrations between the components during the interaction with a segment-based penalty formulation.

Table 5. Contacts between components assigned for the test.

Subsystem 1	Subsystem 2	LS DYNA CARD Selected
Tires	Catapult	CONTACT_AUTOMATIC SURFACE TO SURFACE
Vehicle	Floor	CONTACT_AUTOMATIC SURFACE TO SURFACE
Rear seat	Child dummy	CONTACT_AUTOMATIC SURFACE TO SURFACE
Seatbelt	Child dummy	CONTACT_AUTOMATIC SURFACE TO SURFACE
Mechanical coupling	Child dummy	CONTACT_AUTOMATIC SURFACE TO SURFACE
Mechanical coupling	Rear seat	CONTACT_AUTOMATIC SURFACE TO SURFACE

A static friction coefficient of 0.3 and dynamic friction of 0.2 between the rear seat, the LBB, and the Hybrid III 6yo are defined for the contacts [39]. The static and dynamic coefficients between the vehicle and the concrete are both 0.85 [40].

The VDR-b is fixed to the rear seat, and a translational joint is implemented to allow displacement along the *y*-axis between the VDR-b and the LLDR-b. A cylindrical joint

is selected for the M1, M2, and C displacement on riel T along the *x*-axis. J1, J2, and T implemented a translational joint to allow M1, M2, and C to move along the *z*-axis with respect to J1.

The rear seat vehicle has a contact CONTACT_AUTOMATIC_SURFACE_TO_SURFACE between the seat back and seat cushion structure with the padding (foam). The polypropylene connector connects the seatback with the seat cushion using a Constrained Nodal Rigid Body (CNRB).

3. Results

The time applied for the rollover test was 1 s, with data recording every 1 ms. A comparative kinematics behavior study is carried out between the numerical test by Cruz et al. [25], which considered a six-year-old child positioned in a rear seat with a Low Back Booster (LBB) and anchored with an ISOFIX system (LBB-ISOFIX) and the proposal HDS coupling with a LBB denominated as HDS-LBB. Both studies start at t = 0 ms and end at t = 1000 ms. Figure 6 shows the kinematics difference between both numerical rollover tests.
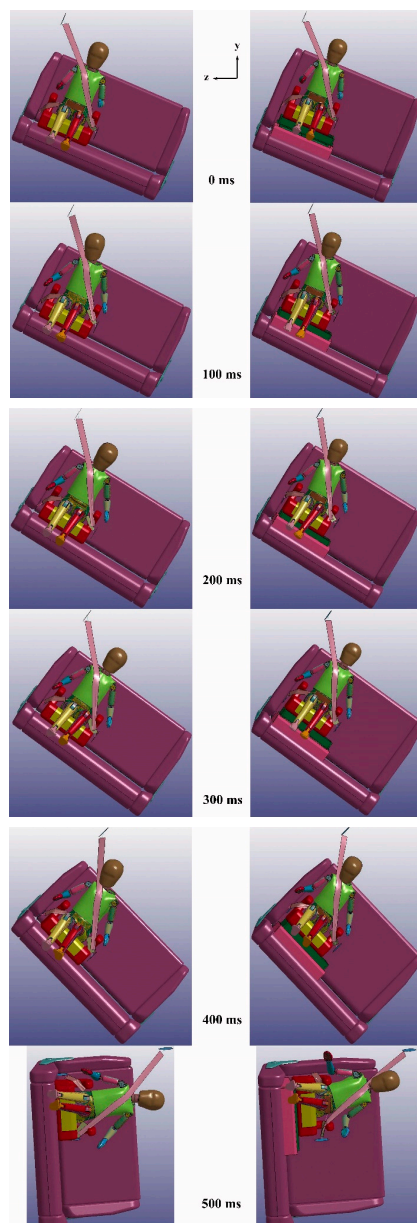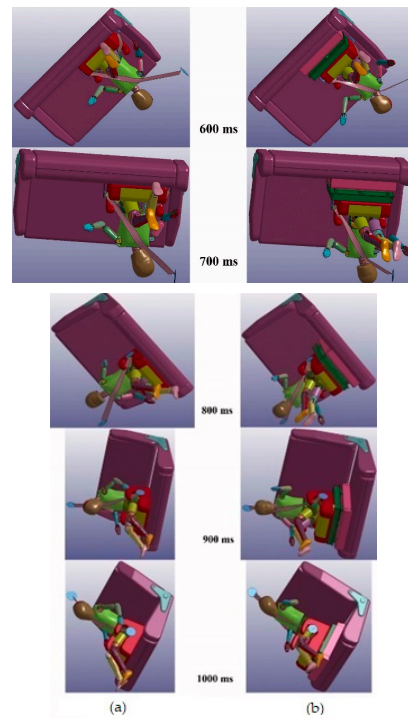

Figure 6. *Cont.*

Figure 6. Dummy kinematics results: (**a**) LBB with ISOFIX by Cruz et al. [25]. (**b**) Harmonic Device System with LBB.

3.1. Head

The child's head-resulting accelerations are obtained and compared to the values reported by Cruz et al. [25] during the numerical rollover established. Figure 7 shows that the most severe accelerations start at 400 ms when the vehicle begins to rotate. For the LBB-ISOFIX at 435 ms, the maximum acceleration of 44.3 occurred, which generated an HIC_{15} of 156. The HDS-LBB reached the maximum acceleration at 440 ms, and 0.4 G was reduced, resulting in a lower HIC_{15} of 128.
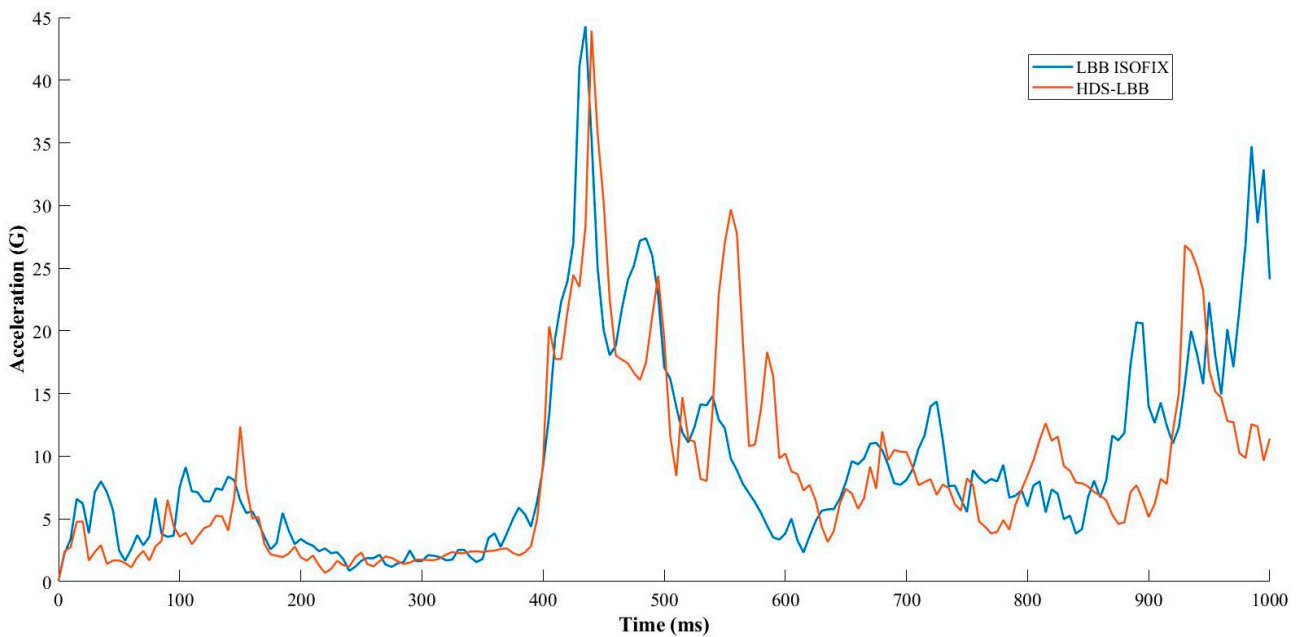

Figure 7. Head resultant accelerations.

With the head accelerometer, the rotational movement in degrees with respect to the neck base is obtained. The maximum flexion reached with the LBB-ISOFIX is 41°, while the HDS-LBB generates a 24° greater, and the extension is reduced by 3°. However, when implementing the HDS-LBB, only three flexion-extension variations are reported, and four variations are observed for the LBB-ISOFIX (Figure 8). These variations are the ones that produce the most significant neck injuries due to the abrupt neck movement displacements from forward to backward and vice versa.
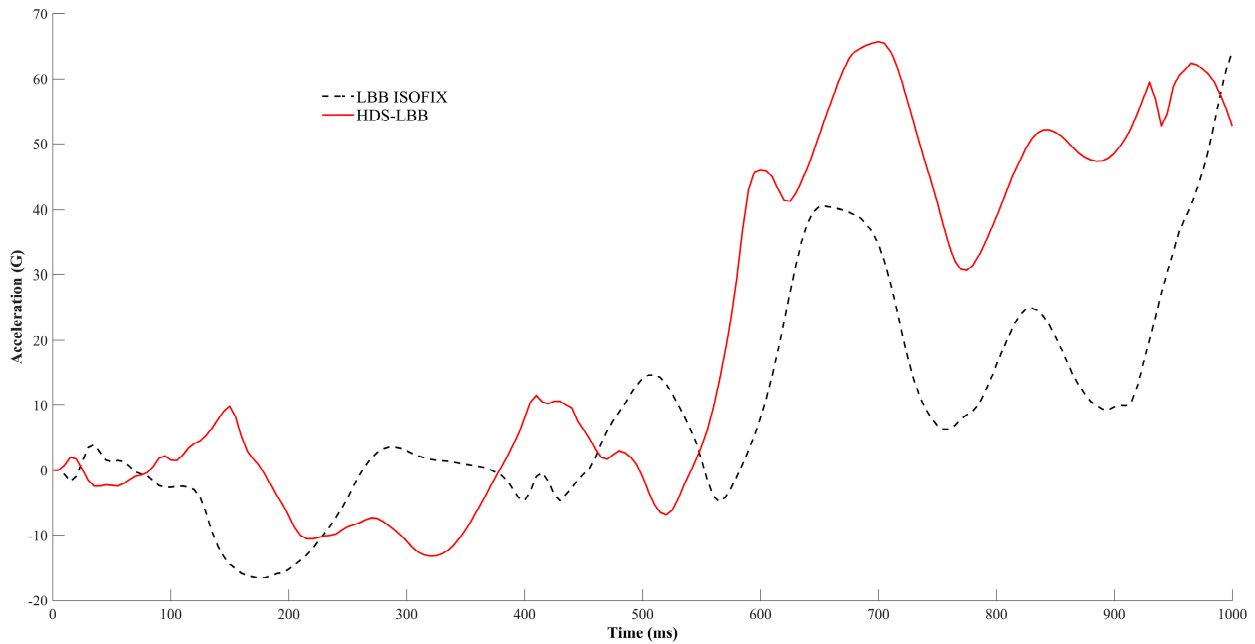

Figure 8. Neck flexion and extension.

The Neck Injury Criteria (N_{ij}) show that both systems remain within the critical values established by NHTSA, so neither causes serious injuries. However, when the HDS-LBB is implemented, it generates more significant extension and compression in the child's neck. The maximum values reached are 26.86 Nm and 404.41 N, respectively (Figure 9).
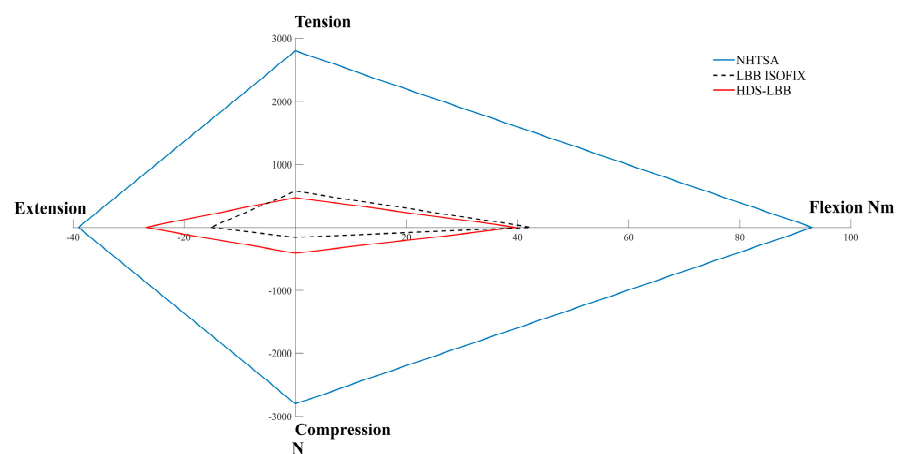

Figure 9. Neck injury criteria (Nij).

3.2. Thorax

Figure 10 shows the thoracic spine accelerations obtained for both configurations. Initially, it can be observed that due to the displacement, the HDS-LBB does not generate decelerations; instead, the LBB-ISOFIX decelerations are measured since the seatbelt began to retain the child. During rollover at 410 ms, the HDS-LBB generates a maximum

acceleration of 58 G and a Chest Severity Index (CSI) of 1518, and at 460 ms, another peak acceleration is reported of 42 G. On the other hand, in the LBB-ISOFIX proposal, the maximum acceleration during a rollover is 25 G, and the CSI is 425.2. NHTSA establishes a Clip3m metric with a value of 60 before the injury threshold begins. The value obtained with the HDS-LBB is 55.12, and the LBB-ISOFIX decreases to 27.94.
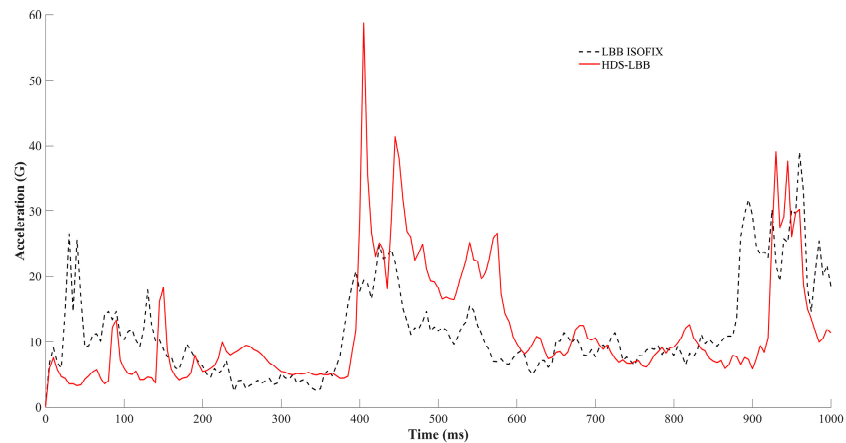

Figure 10. Thoracic spine resultant acceleration.

The thoracic spine deflections generated with the HDS-LBB are 16 mm and keep oscillating from 4 to 14 mm. With the LBB-ISOFIX, the deflection does not exceed 5 mm during the one-second interval. NHTSA establishes a thoracic spine deflection of 40 mm for a 6-year-old child, so despite the increase caused by the mechanical coupling with LBB, no damage is generated in the child (Figure 11).
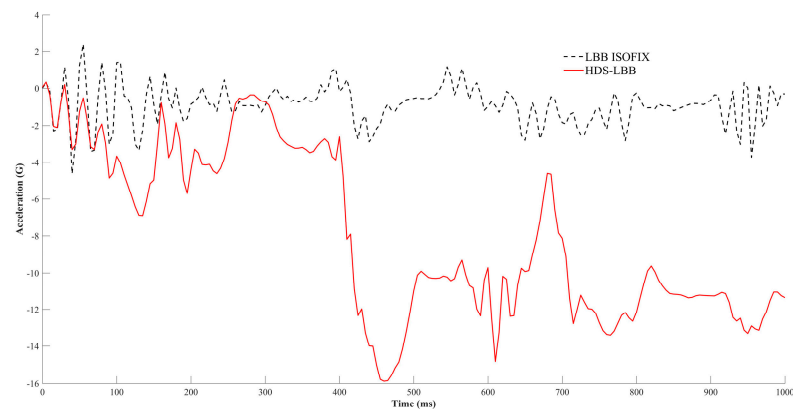

Figure 11. Thoracic spine deflection.

4. Discussion

HDS-LBB is shown to be less effective in the interval 400–700 ms due to the children suffering a seatbelt interaction with the neck.

The numerical analysis results for the HDS-LBB were compared to the findings presented by Cruz et al. [25], who evaluated three case studies during rollovers. The seat vehicle, the Hybrid III six years old, and the LBB are modeled using the same techniques and parameters as Cruz et al. [25]. The HDS-LBB and the LBB-ISOFIX rollover tests considered no pretensioner or retractor for the seatbelt. Some limitations included that the test was performed only in a sedan vehicle (Yaris 2010) and a six-year-old child, additional test needed to be performed with different vehicles such as SUVs or trucks, and with another child ATD as a three-year-old to assess the feasibility of its use with other age groups of children according to the UN/ECE R129.

Table 6 shows the IARV values established by different regulators and the values obtained. In both scenarios, the LBB-ISOFIX and the HDS-LBB remained below the IARVs established by the NHTSA and the European Enhanced Vehicle-Safety Committee (EEVC) [41,42]. According to the results, the head and thorax do not present the possibility of suffering a higher injury risk than AIS 3. The injury risk reported has some limitations because these were reported from data obtained by frontal accidents, and IARVs do not exist for a rollover crash. However, body regions such as the head and thorax can be evaluated with this IARVS due to HIC_{15} is measured into X, Y, Z axes, and chest deflection can be measured in the direction of interest. N_{ij} was not considered in this case because the values reported by the HDS-LBB show small values during the rollover. The head–neck region has a non-linear trajectory, so the forces applied to the neck not only have extension and flexion movements but also have forces and moments in several axes. Thorax acceleration represents an AIS injury risk lower than AIS 3 as a result of NHTSA IARVS limits.

Table 6. Comparative Injury Assessment Reference Values (IARVs) according to different reports and the values obtained in the numerical simulations.

| | | Injury Metrics | | | IARVS | | |
| | | Values from the Numerical Simulations Performed | | | | EEVC [42] | |
	Units	HDS-LBB	LBB-ISOFIX	NHTSA Threshold [41]	UN R94	AIS > −3 20% LR	AIS > −3 50% LR
HIC_{15}	---	144	156	700	986	1083	1389
N_{ij}	---	0.833 TE	0.443—TE 0.660—TF 0.510—CE 0.594—CF	1	---	---	---
Neck force (F_z)	N	404.41 ^{T}	150.64	2800 ^{T} 2800 ^{C}	1824	2101	2304
Neck moment (M_y)	Nm	26.86 ^{E}	15.17	93 ^{F} 39 ^{E}	94	118	143
Chest deflection	mm	14	5	40	42	33	49
Thorax acceleration	G's	58	25	60	---	---	---

T—Neck Tension Force; C—Neck Compression Force; F—neck moment in flexion; E—neck moment in extension.

The increment in the neck and thorax values occurred as the seatbelt slid across the child's shoulder during lateral movement along the *z*-axis and vertical movement along the *y*-axis, affecting the effectiveness of the CRS. The HDS-LBB configuration used in the numerical rollover crash test does not allow a correct interaction of the vehicle's seatbelt with the thorax because the seatbelt height can be corrected in the Toyota Yaris Sedan 2010, so the numerical model looks to imitate this behavior. The height increment by the HDS-LBB originates that the shoulder belt can be positioned over the sternum, increasing the slipping seat belt risk to the neck and increasing the injury risk for some body regions. This behavior is shown during the kinematics results obtained by the rollover test. An alternative way to reduce child injuries is the HDS-LBBB embedded into the rear seat. With this modification, shoulder belt positioning may result in an optimal belt geometry setting.

The HDS-LBB model resulted in a 72% increase in the peak value of the thorax injury. The $Clip_{3m}$ measured a value of 55.12 G's, while the deflection reached 16 mm. In terms of neck injuries, the Neck Injury Criteria (Nij) indicated a more significant extension, reaching 26.86 Nm and compression of 404.41 N. It is important to note that despite the increase in neck and thorax injuries caused by the HDS-LBB model, these injuries remained below the NHTSA threshold. The study highlights that while the HDS-LBB attempts to dissipate energy during crashes, a seatbelt slipping can lead to increased child injury.

Another potential solution involves implementing a system that allows the seatbelt to move in accordance with the HDS-LBB's trajectory, preventing the seatbelt from slipping. However, the feasibility of this solution requires further verification through additional numerical studies and laboratory test procedures, as well as considerations of economic viability.

5. Conclusions

It is essential to introduce a Child Restraint System to enhance child safety during rollovers that can protect groups 1, 2, and 3 according to UN/ECE Regulation R44 to offer better protection to a wider age range and different anthropometric characteristics. Commonly, the CRSs indicate which body weight or height is suitable. Also, the anchor system is approved for every country, but several semi-universal CRSs need to be checked to ensure it is compatible with seat vehicles. The HDS-LBB offers an alternative anchor system to seat vehicles from different countries, so the limitations of some CRS can be fulfilled. A Low Back Booster (LBB) with ISOFIX ensures proper seatbelt positioning for the child, while ISOFIX anchors securely fasten the LBB to the vehicle seat, minimizing the risk of seatbelt slippage-related injuries for group 2. While the implementation of a HDS offers the same anchor security to the LBB, it is observed according to the result that the mechanism can decrease the energy transferred to the child, but the HDS needs more tests with different vehicles and different child dummies due to it was observed that the seatbelt slips in some time interval and this effect needs to be avoided. The seatbelt synchronization with the HDS is crucial for more efficient energy dissipation without increasing the child's vulnerability to injuries during rollovers.

References

1. Instituto Nacional de Estadística y Geografía (INEGI). Accidentes Por Tipo. 2023. Available online: https://www.inegi.org.mx/app/tabulados/interactivos/?pxq=ATUS_ATUS_4_63710dee-dbe8-45f2-b71b-01b7970b0966 (accessed on 2 August 2023).
2. National Highway Traffic Safety Administration. *Review of NMVCCS Rollover Variables in Support of Rollover Recon-Struction [DOT HS 811 235]*; National Highway Traffic Safety Administration: Washington, DC, USA, 2010.
3. El-Menyar, A.; Latifi, R.; Parchani, A.; Peralta, R.; Tuma, M.; Zarour, A.; Abdulrahman, H.; Al-Thani, H.; Asim, M.; El-Hennawy, H. Epidemiology, Causes and Prevention of Car Rollover Crashes with Ejection. *Ann. Med. Health Sci. Res.* **2014**, *4*, 495. [CrossRef] [PubMed]
4. George, R.; John, L. *Rollover Crash Study Vehicle: Design and Occupant Injuries*; Monash University: Melbourne, Australia, 1994.
5. Liu, S.; Fan, W.D.; Li, Y. Injury Severity Analysis of Rollover Crashes for Passenger Cars and Light Trucks Considering Temporal Stability: A Random Parameters Logit Approach with Heterogeneity in Mean and Variance. *J. Saf. Res.* **2021**, *78*, 276–291. [CrossRef] [PubMed]
6. *J2114_201102*; SAE International Recommended Practice, Dolly Rollover Recommended Test Procedure. SAE Standard: Warrendale, PA, USA, 1993. [CrossRef]
7. National Highway Traffic Safety Administration. *Laboratory Test Procedure for FMVSS 208-14-Occupant Crash Protection*; National Highway Traffic Safety Administration: Washington, DC, USA, 2008.
8. Whitman, G.; Sicher, L.; Yannaccone, J.; Hooker, R. *Dolly Rollover Testing of Child Safety Seats*; SAE Technical Paper 2006-01-0914; SAE International: Warrendale, PA, USA, 2006. [CrossRef]
9. Durbin, D.R.; Jermakian, J.S.; Kallan, M.J.; McCartt, A.T.; Arbogast, K.B.; Zonfrillo, M.R.; Myers, R.K. Rear Seat Safety: Variation in Protection by Occupant, Crash and Vehicle Characteristics. *Accid. Anal. Prev.* **2015**, *80*, 185–192. [CrossRef] [PubMed]

10. Myers, R.K.; Lombardi, L.R.; Pfeiffer, M.R.; Curry, A.E. Restraint Use Characteristics among Crash-Involved Child Passengers: Identifying Opportunities to Enhance Optimal Restraint Use. *Traffic Inj. Prev.* **2022**, *23*, S213–S217. [CrossRef] [PubMed]

11. Benedetti, M.; Klinich, K.D.; Manary, M.A.; Flannagan, C.A.C. Factors Affecting Child Injury Risk in Motor-Vehicle Crashes. *Stapp Car Crash J.* **2020**, *63*, 195–211.

12. Durbin, D.R.; Chen, I.; Smith, R.; Elliott, M.R.; Winston, F.K. Effects of Seating Position and Appropriate Restraint Use on the Risk of Injury to Children in Motor Vehicle Crashes. *Pediatrics* **2005**, *115*, e305–e309. [CrossRef] [PubMed]

13. García-España, J.F.; Durbin, D.R. Injuries to Belted Older Children in Motor Vehicle Crashes. *Accid. Anal. Prev.* **2008**, *40*, 2024–2028. [CrossRef] [PubMed]

14. Valent, F.; McGwin, G.; Hardin, W.; Johnston, C.; Rue, L.W. Restraint Use and Injury Patterns among Children Involved in Motor Vehicle Collisions. *J. Trauma Inj. Infect. Crit. Care* **2002**, *52*, 745–751. [CrossRef] [PubMed]

15. Rivara, F.P. Injuries and Death of Children in Rollover Motor Vehicle Crashes in the United States. *Inj. Prev.* **2003**, *9*, 76–80. [CrossRef] [PubMed]

16. Center for Child Injury Prevention Studies. Injury Risk and Causation Scenarios of Children Involved in Rollover Crashes. Available online: https://cchips.research.chop.edu/injury-risk-and-causation-scenarios-of-children-involved-in-rollover-crashes (accessed on 6 December 2023).

17. Martínez-Miranda, M.A.; Torres San Miguel, C.R.; Flores-Campos, J.A.; Ceccarelli, M. *Numerical Simulation of a 2D Harmonic Oscillator as Coupling System for Child Restraint Systems (CRS). Mechanisms and Machine Science*; Springer: Cham, Switzerland, 2021; Volume 91, pp. 492–502. [CrossRef]

18. Cruz-Jaramillo, I.L.; Martínez-Sáez, L.; Torres-SanMiguel, C.R. Numerical Simulation of Mechanical Coupling for Low-Back Booster with a 6-Year-Old Child during a Crash Test. *Appl. Sci.* **2022**, *12*, 5350. [CrossRef]

19. Holdampf, C.J.; Vangipuram, R. Vehicle Seat Interlock System. U.S. Patent No. 5,603,550, 18 February 1997. pp. 1–19.

20. Lane, W.C., Jr. Apparatus with a Child Seat and an Energy Absorption Mechanism. U.S. Patent No. 5,685,603, 11 November 1996, pp. 1–20.

21. Amesar, P.T.; Nakhla, S.; Przybylo, P.; Tobin, J.R. Energy Absorbing Tether for Child Safety Seat. U.S. Patent US-20090026815-A1, 28 January 2008.

22. Wang, H. Energy Absorbing and Damping Device for Child Car Seat. European Patent EP3040234B1, 26 December 2013.

23. Van Der Veer, E.; Van Mourik, O.; Van Houtert, R. Rotating Child Safety Seat. JUSTIA Patent 20130154318, 9 September 2012.

24. Graham, S. *Fundamentals of Mechanical Vibrations*, 2nd ed.; McGraw-Hill: New York, NY, USA, 2016.

25. Cruz-Jaramillo, I.L.; Torres-San Miguel, C.R.; Martínez-Sáez, L.; Ramírez-Vela, V.; Urriologoitia-Calderón, G.M. Numerical Low-Back Booster Analysis in a 6-Year-Old Infant during a Dolly Rollover Test. *J. Adv. Transp.* **2020**, *2020*, 5803623. [CrossRef]

26. Marzougui, D.; Radwan, R.; Cui, C.; Kan, C.-D.; Opiela, K.S. Extended Validation of the Finite Element Model for the 2010 Toyota Yaris Passenger Sedan. In Proceedings of the Transportation Research Board 92nd Annual Meeting, Washington, DC, USA, 13–17 January 2013.

27. Carrero, A. *Simulación de Un Choque Lateral Con Dummy Con Cinturón Mediante LS-DYNA*; Universidad Carlos III de Madrid Escuela Politécnica Superior: Madrid, Spain, 2011.

28. Kang, S.; Chen, C.; Guha, S.; Paladugu, M.; Ramasamy, M.S.; Gade, L.; Zhu, F. LS-DYNA Belted Occupant Model. In Proceedings of the 15th International LS-DYNA Users Conference, Detroit, MI, USA, 10–14 June 2018.

29. UNECE. *Regulation No. 129 of the Economic Commission for Europe of the United Nations (UN/ECE)—Uniform Provisions Concerning the Approval of Enhanced Child Restraint Systems Used on Board of Motor Vehicles (ECRS)*; UNECE: Geneva, Switzerland, 2018.

30. UNECE. *UN Regulation No. 129 Increasing the Safety of Children in Vehicles*; UNECE: Geneva, Switzerland, 2016.

31. Callister, W.D.; Rethwisch, D.G. *Materials Science and Engineering: An Introduction*, 10th ed.; Wiley: Hoboken, NJ, USA, 2018.

32. Tay, Y.Y.; Lim, C.S.; Lankarani, H.M. A Finite Element Analysis of High-Energy Absorption Cellular Materials in Enhancing Passive Safety of Road Vehicles in Side-Impact Accidents. *Int. J. Crashworthiness* **2014**, *19*, 288–300. [CrossRef]

33. Beer, F.P.; Johnston, E.R.; DeWolf, J.T. *Mecánica de Materiales*, 8th ed.; McGraw Hill: New York, NY, USA, 2021.

34. Hibbeler, C. *Mecánica de Materiales*, 9th ed.; Pearson: London, UK, 2017.

35. Alamsyah; Sari, F.I.; Arifuddin, A.M.N.; Pawara, M.U.; Mubarak, A.A. Experimental Test of Tensile Strength of Barge Deck Plate Welded Joints. *Int. J. Metacentre* **2022**, *2*, 9–17.

36. Chung, C.-H.; Choi, H.; Park, J. Local Collision Simulation of an SC Wall Using Energy Absorbing Steel. *Nucl. Eng. Technol.* **2013**, *45*, 553–564. [CrossRef]

37. Lee Spring Resortes de Compresión. Available online: https://www.leespring.mx/es/resortes-de-compresion (accessed on 1 August 2023).

38. DICTATOR. Amortiguadores de Impacto DICTATOR. Available online: https://dictator.es/herrajes-y-accionamientos/amortiguadores-hidraulicos/amortiguadores-de-impacto/amortiguadores-de-impacto#:~:text=Los%20amortiguadores%20de%20impacto%20de,en%20ambos%20lados%20(ZDH) (accessed on 1 August 2023).

39. Gavelin, A.; Lindquist, M.; Oldenburg, M. Modelling and Simulation of Seat-Integrated Safety Belts Including Studies of Pelvis and Torso Responses in Frontal Crashes. *Int. J. Crashworthiness* **2007**, *12*, 367–379. [CrossRef]

40. Reed, W.S.; Keskin, A.T. *Vehicular Deceleration and Its Relationship to Friction*; SAE Technical Paper 890736; SAE International: Warrendale, PA, USA, 1989. [CrossRef]

41. Eppinger, R.; Sun, E.; Bandak, F.; Haffner, M.; Khaewpong, N.; Maltese, M.; Kuppa, S.; Nguyen, T.; Takhounts, E.; Tannous, R.; et al. *Development of Improved Injury Criteria for the Assessment of Advanced Automotive Restraint Systems-II*; National Highway Traffic Safety Administration: Washington, DC, USA, 1999.

42. Wismans, J.; Waagmeester, K.; Le Claire, M.; Hynd, D.; De Jager, K.; Palisson, A.; van Ratingen, M.; Trosseille, X. *Q-Dummies Report: Advanced Child Dummies and Injury Criteria for Frontal Impact*; EEVC: London, UK, 2018.